



# Sol–Gel Synthesis, Structure Characterization and Optical Properties of NiO-CuO Nanocomposite

B. S. Satavekar

Department of Chemical Engineering

Tatyasaheb Kore Institute of Engineering and Technology, Warananagar.

Warananagar, MS-India - 416113

S. V. Anekar

Department of Chemical Engineering

Tatyasaheb Kore Institute of Engineering and Technology, Warananagar.

Warananagar, MS-India-416113

\* B. S. Shirke

Department of Chemistry

Yashwantrao Chavan Warana Mahavidyalaya, Warananagar,

Warananagar, MS-India-416113

## Abstract

A new NiO-CuO nanocomposite has been successfully synthesized by a sol-gel method using nickel chloride hexahydrate, copper chloride hexahydrate, ammonia and ethylene glycol as a precursors. The resulting material was characterized by XRD, SEM, TEM, EDAX, UV-Visible, FTIR, and TGA-DTA techniques. XRD analysis revealed all the relevant Bragg's reflections for face-centered cubic and monoclinic structure of NiO-CuO. The average particle size was obtained 25 nm by using the Scherrer equations. The value of particle size determined from XRD was in good agreement with the SEM and TEM analysis. The direct optical band gap was found to be at 3.3 eV. Furthermore, the thermal behaviour of mixed salts has been studied using thermal analysis (TG and DTA). To verify the purity of the composites and the elemental composition of the constituent oxides checked by FTIR and EDAX were performed.

**Keywords** - Sol-gel, Metal Oxide, Nanocomposite, semiconductors, Thermal

\*Corresponding Author: Dr. B. S. Shirke, Material Science Laboratory, Department of Chemistry, Y.C. Warana Mahavidyalaya, Warananagar, Maharashtra, India-416113.

## 1. Introduction

Now a day, the research in materials science is very active. Material science finds widespread application in engineering, technology and science. These materials include ceramics, polymers, semiconductors, magnetic materials and biomaterials etc. Nanotechnology is a rapidly emerging scientific subject in materials science that produces and constructs gadgets that are valuable to society for technical improvement [1]. Nanomaterials have special qualities include enhancing the electrical conductivity, ductility, toughness, and formability of ceramics, enhancing the hardness and strength of metals and alloys, and enhancing the luminous efficiency of semiconductors. It utilized to produce lightweight industrial applications with a high surface area to volume ratio, enhancing the functionality of electronics and information technology, enabling the use of more sustainable energy sources, and playing a crucial role in environmental remediation applications [2].

A composite material is a mixture made up of at least two phases with differing chemical compositions. A significant class of materials in the field of nanotechnology is going to be metal-polymer or metal oxide-polymer nanocomposites. From a theoretical and practical perspective, it has been really interesting. Such materials' properties can be combined to create materials that respond as desired. When particle sizes are reduced to extremely small dimensions, optical or magnetic characteristics may alter. These properties

are generally of great interest in the field of nanocomposite materials. Composites have excellent properties like high hardness, high melting point, low density, low coefficient of thermal expansion, high thermal conductivity, good chemical stability, and improved mechanical properties like higher specific strength, better wear resistance, and specific modulus. They also have good potential for various industrial fields like sensors and energy conversion [3].

The performance of hybrid nanostructured materials' is primarily influenced by their size, shape, composition, structure, crystal phases. Controlled synthesis of hybrid metal oxide nanostructures is therefore crucial in order to achieve the required size, shape, and structure of the hybrid nanostructure [4]. There are several ways for preparing nanocomposites, including homogeneous precipitation, co-precipitation, thermal decomposition, and hydrothermal processes, but the sol-gel method has been widely employed for preparing inorganic oxide nanocomposites [5]. The conventional approach for preparing the oxide is usually the ceramic route; however, the sol-gel route offers numerous advantages, such as good homogeneity, fewer process steps, ease of remote operation, low sintering temperature, and more [6].

Nanoscale transition metal oxide semiconductors are very much in demand, due to their physical, biological, and chemical properties. This increases their application in a number of modern science and technology disciplines, as well as their ability to improve the environment and human health [7]. Mixed transition metal oxide (MTMO) has gained popularity in recent years as a potential material for numerous applications in electro catalysis, sensing, charge storage, and catalysis. The active surface area and charge transfer efficiency of MTMO nanocomposites are increased, which enhances the electrochemical performance [8]. The development of metal oxide nanoparticles using green synthesis techniques is the subject of current study, which also offers a low-cost, economical method [9]. Researchers have looked into mixed catalysts in heterogeneous catalysis, which may be more effective than their individual parts [10].

Cupric oxide (CuO) is an inherently p-type semiconductor with a small band gap ranging from 1.2 eV to 3.57 eV. It has monoclinic structure and unique properties such as super thermal conductivity, photovoltaic properties, high stability, and antimicrobial activity. CuO is used in a variety of applications, including photodetectors, photocatalysis, gas sensors, and solar cells [11-13].

Nickel Oxide (NiO) is a green crystalline solid exhibits ferromagnetic properties and has a Neel temperature of 523 K. NiO nanostructures are p-type semiconductors with unique magnetic and electric properties that are depend on particle size. The band gap of NiO semiconductor is ranging between 3.6-4.0 eV and is known for its exceptional chemical stability. Due to low cost and excellent ion storage property, it has become an attractive research material [14-16].

There are several reports in the literature of NiO-CuO powder preparation by microwave processing. Samreen Zahra et al. revealed that crystals of NiO and CuO nanoparticles aggregated to form spheres of variable sizes were successfully embedded in the amorphous silica matrix composed of silica particles agglomerated to form clusters [17]. Sujit Chatterjee et al. reported the particle dimension can be reduced and porosity may be increased by suitable modification of the synthesis protocol and better fabrication for more efficient devices [18]. L. Argueta-Figueroa reported that, good alternative metal oxide materials such as nickel oxide (NiO), copper oxide (CuO), manganese oxide, and cobalt oxide for highly costly noble metals such as gold (Au), platinum (Pt), lead (Pb), and palladium (Pd). Among these relatively low-cost metal oxides, NiO and CuO are of particular importance owing to their good electrochemical stability and activity [19].

In the present study, we synthesized NiO-CuO nanocomposite by cost effective sol-gel route and characterized using techniques XRD, SEM, TEM, UV-DRS, TGA and FT-IR.

## 2. Experimental Details

### 2.1. Materials and Chemicals

All chemicals used in this experiment were of reagent grade and used without any further purification. Nickel chloride hexahydrate ( $\text{NiCl}_2 \cdot 6\text{H}_2\text{O}$ ), copper chloride hexahydrate ( $\text{CuCl}_2 \cdot 6\text{H}_2\text{O}$ ), ammonia ( $\text{NH}_4\text{OH}$ ) and ethylene glycol procured from Sigma Aldrich were used as the precursors. All the glasswares which were utilized appropriately cleaned afterwards washed with distilled water. Deionized water has been used as the solvent throughout the synthesis.

### 2.2. Synthesis of NiO-CuO Nanocomposites

CuO doped NiO nanocomposite were prepared according to the formula  $\text{Ni}_x\text{Cu}_{1-x}\text{O}$  ( $X = 0.1$ ). After mixing the appropriate amounts of (0.1M) precursor's solutions, aqueous ammonia (0.1M) was added drop wise with constant stirring to adjust the pH value at 10-11. After adjusting pH, the obtained green precipitate was washed with deionized water to remove formed by products during the reaction process. When the solution became neutral, it was dried at  $100^\circ\text{C}$  for 24 hours. The grinding of particles into a fine powder using agate pestle mortar followed complete drying. The fine powder was subjected to 4 hours annealing at  $400^\circ\text{C}$  to obtain NiO-CuO nanocomposites.

### 2.3. Characterization of Nanocomposite Material

The X-ray diffraction of the powder materials was measured on Siemens, D-500 diffractometer with Cu-K $\alpha$  ( $\lambda = 1.5406 \text{ \AA}$ ) operating at 45 kV and 100 mA over a range of  $2\theta$  angle from  $10^\circ$  to  $80^\circ$ , at a scanning rate of  $5^\circ/\text{min}$ . The UV-Visible (UV-Vis) absorption spectra were recorded in a 'Jasco (model V-770) UV-Vis-NIR Spectrophotometer' in the wavelength scale varied from 200 to 800 nm. Transmission Electron Microscope (TEM) studies of the powder sample was carried out by using model: JEOL JEM 2100 plus, Japan. Thermogravimetric analysis/ Differential thermal analysis/ Differential scanning calorimetry were recorded by using model: SDT Q600, make: TA Instrument USA. A Fourier transform infrared spectroscopy (FTIR) of sample carried by using model: Agilent Technology Cary 630 FTIR.

## 3. Result and Discussion

### 3.1. X-ray Diffraction

Crystalline structure of materials was identified by x-ray diffraction method. Figure.1 shows XRD pattern of sample, it clearly indicating the formation of crystalline NiO-CuO nanocomposite material. The diffraction peaks of NiO-CuO nanocomposite at  $32.46^\circ$ ,  $35.52^\circ$ ,  $38.72^\circ$ ,  $48.80^\circ$ ,  $53.42^\circ$ ,  $58.23^\circ$ ,  $61.57^\circ$ ,  $66.12^\circ$ ,  $68.08^\circ$ , and  $72.35^\circ$  closely match with the planes (110), (002), (111), (-202), (020), (202), (022), (-113), (-311) and (113) good agreement with ( JCPDS No. 89–5899) corresponds to the end-centered monoclinic structure of CuO and the diffraction peaks at  $37.19^\circ$ ,  $43.23^\circ$ ,  $62.80^\circ$ ,  $75.24^\circ$  and  $79.28^\circ$  closely match with the (111), (200), (220), (311) and (222) crystalline planes and were indexed to face-centered cubic structure of NiO as per the (JCPDS No. 78- 0429).

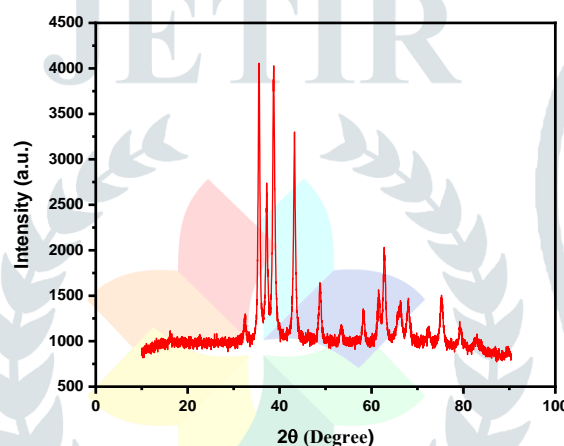


Figure 1. XRD pattern for of NiO-CuO nanocomposite

The effect of CuO nanoparticles on the microstructural properties of the NiO, we have estimated the average crystallite size (D) and the strain ( $\epsilon$ ) present in NiO sample from the full width at half maximum (FWHM) of the XRD peaks by using the following Scherrer equations,

$$D = \frac{k\lambda}{\beta \cos\theta}$$

$$\epsilon = \frac{\beta \cos\theta}{4}$$

where, D is the average crystallite size,  $\epsilon$  the strain,  $\lambda = 1.54056 \text{ \AA}$  is the wavelength of Cu  $k\alpha$ ,  $\beta$  is the full width at half-maximum intensity,  $\theta$  is Bragg's diffraction angle, and K is a constant taken as to 0.94.

The values of D and  $\epsilon$  estimated from XRD line width were about 25.26 nm and 0.24 % respectively for the NiO-CuO nanocomposites. The lattice constants comprising a, b, and c for the monoclinic structure, and a for the cubic structure were calculated using the following relationships, respectively.

$$\frac{1}{d^2} = \frac{1}{\sin^2\beta} \left( \frac{h^2}{a^2} + \frac{k^2 \sin^2\beta}{b^2} + \frac{l^2}{c^2} - \frac{2hl \cos\beta}{ac} \right)$$

$$\frac{1}{d^2} = \left( \frac{h^2 + k^2 + l^2}{a^2} \right)$$

The lattice parameters calculated from the present data are  $a = 4.68 \text{ \AA}$ ,  $b = 3.43 \text{ \AA}$ , and  $c = 5.14 \text{ \AA}$  for CuO, and  $a = 4.19 \text{ \AA}$  for NiO.

### 3.2. Scanning Electron Microscopy (SEM)

Superficial morphological properties, particle size dispersal and surface texture of nanocomposite materials were examined by scanning electron microscopy. The sol-gel synthesized nanocomposite image is shown in figure 2. From the image particles are revealed as relatively agglomerated and it shows nanoflower like morphology. The average particle size is about 25 nm. The morphological study shows that the material is mesoporous in nature. The porous nature material allows more surface active sites for adsorption. The particle size of nanocomposites noticed from SEM is like to be calculated from XRD

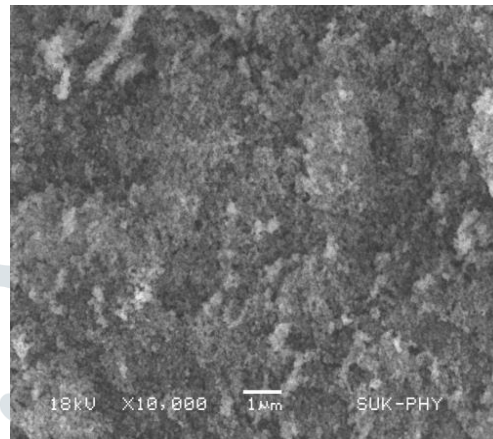


Figure 2. SEM image for of NiO-CuO nanocomposite

### 3.3. Transmission Electron Microscopy (TEM)

TEM analysis gives information about size and morphology of materials. To gain more information on the interior microstructure and crystallographic properties of the nanocomposites, TEM image in figure 3 presents spherical and cubic structure of NiO-CuO nanocomposite. The interconnection between nanoparticles is an indication of the formation of mesoporous structure. It shows spherical agglomerated nanoparticles. The results clearly show that the mean particle size estimated by TEM is in good agreement with the average crystallite size determined from the XRD data.

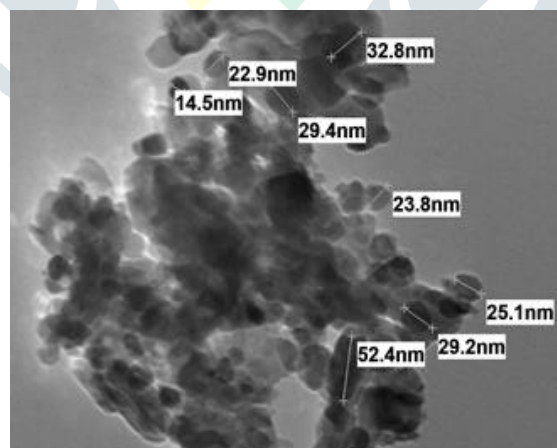
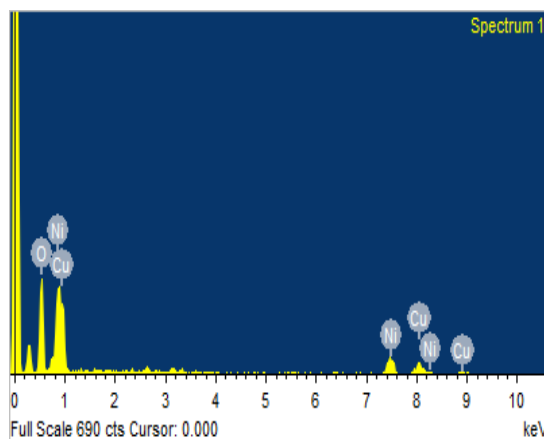


Figure 3. TEM image for of NiO-CuO nanocomposite

### 3.4. Energy-Dispersive X-ray Spectroscopy

EDX analysis was used to investigate the chemical composition of the synthesized samples. The obtained EDX spectrum are shown in figure 4. The EDX spectrum of NiO-CuO nanocomposite confirms the presence of Ni, Cu and O elements in this sample with no other impurity peaks. The EDX spectrum present the high content of oxygen in the nanocomposites.



**Figure 4. EDX image for of NiO-CuO nanocomposite**

### 3.5. UV-Vis DRS Spectral Study

To determine the optical property of prepared nanocomposite, diffuse reflectance spectrum of the was investigated using UV-Visible optical spectroscopy in the range of 200 nm to 800 nm. It is shown in figure 5 a. Diffuse reflectance spectroscopy (DRS) analysis of absorbing material is based on Tauc formula as given below,

$$\alpha h\nu = B (h\nu - E_g)^n$$

where,  $\alpha$  ( $2.303A/d$ ) is the coefficient of absorption,  $A$  is the absorbance,  $d$  is the optical path length,  $B$  is proportionality constant,  $E_g$  is the band gap energy,  $h\nu$  is the energy of photon and  $n$  is a constant which is found to be  $\frac{1}{2}$  for direct allowed transitions and 2 for indirect allowed transitions. The value of optical band gap of the prepared sample was calculated using Tauc plot by plotting  $(\alpha h\nu)^2$  versus  $(h\nu)$  is 3.3 eV shown in figure 5 b.

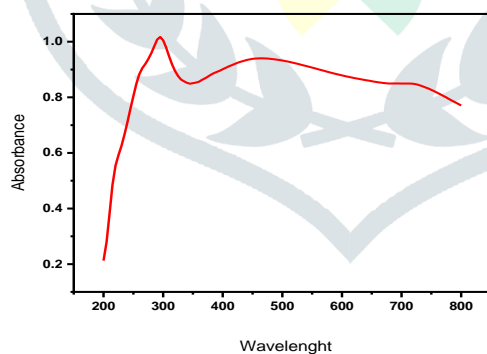


**Figure 5 a. UV-Visible absorption spectrum of NiO-CuO nanocomposite**

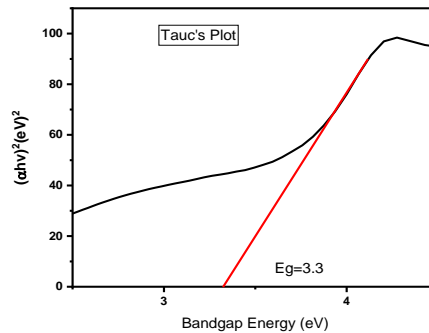


Figure 5 b. Tauc plot of NiO-CuO nanocomposite

### 3.6. Fourier Transform Infrared Spectroscopy (FTIR)

Fourier transform infrared spectroscopy (FTIR) was used to identify the characteristic functional groups in the samples. The FTIR spectrum of NiO-CuO composites are shown in figure 6. The prepared sample reveal the presence of some absorption bands in the ranges from  $400\text{ cm}^{-1}$  to  $4000\text{ cm}^{-1}$ .

The broad absorption peak was observed at around  $3443\text{ cm}^{-1}$  corresponding to O–H stretching. The bands at  $2922.78$  and  $2856.74\text{ cm}^{-1}$  are due to bending vibrations of C–H bond. The peaks at  $1629\text{ cm}^{-1}$  and  $1387\text{ cm}^{-1}$  are attributed to the symmetric and asymmetric C=O stretching vibration modes. The intensity of these peaks was found to increase with the increase in Cu doping. The small peak at  $801\text{ cm}^{-1}$  is attributed to C–H stretching. The dip at  $657\text{ cm}^{-1}$  shows the vibrations of metal oxygen metal bond. The peak was observed at  $657.13\text{ cm}^{-1}$  for NiO-CuO nanocomposite due to the presence of Cu–O bond. The strong band observed at  $482.40\text{ cm}^{-1}$  is the stretching vibrational peak of NiO. The observed broad band assigned at  $574.62\text{--}482.40\text{ cm}^{-1}$  of the mixed oxides may be attributed to the M–O vibration. In addition, this broadness is due to existence of nano-particles in the mixed system.

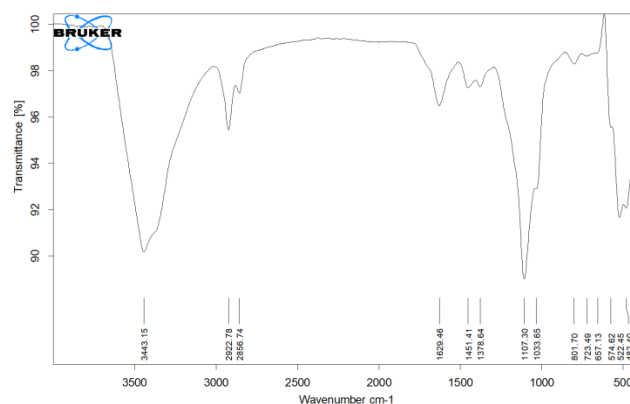


Figure 6. FTIR image of NiO-CuO nanocomposite

### 3.7. Thermo Gravimetric Analysis (TGA)

In order to examine the thermostability of NiO-CuO nanocomposite was directly towards the oxidation and cracking-combustion behaviour, and even further kinetic analysis, which were determined using differential scanning calorimetry (DSC) and thermo gravimetric analysis-differential thermal analysis (TGA-DTA) shown in figure 7. TGA analysis was carried out under air atmosphere from ambient temperature to  $800^\circ\text{C}$ .

From TGA curve, first step evaporation temperature ranges from  $21^\circ\text{C}$  to  $159^\circ\text{C}$ , with a maximum at  $60^\circ\text{C}$ . It was accompanied by a mass loss of about  $0.7508\%$ , which was about  $0.06466\text{ mg}$ . The second stage observed thermal decomposition in the temperature range of  $159^\circ\text{C}$  to  $299.60^\circ\text{C}$ . It was accompanied by a mass loss of about  $0.8689\%$  which was about  $0.07484\text{ mg}$ . The third stage observed the desorption of two carbon dioxide and two nitrogen dioxide molecules at temperature range of  $299.60^\circ\text{C}$  to  $337.94^\circ\text{C}$ . It was accompanied by a mass loss of about  $0.8689\%$  which was about  $0.07484\text{ mg}$ . The fourth stage observed reduction of hydroxides to the oxides by losing two molecules of water between a temperature range  $337.94^\circ\text{C}$  to  $567^\circ\text{C}$ . It is accompanied by a mass loss of about  $0.4133\%$  which was about  $0.03560\text{ mg}$ . The last thermal stable in the temperature range of  $567^\circ\text{C}$  and  $782^\circ\text{C}$  was defined as the region, where the residual polymer chains were burned.

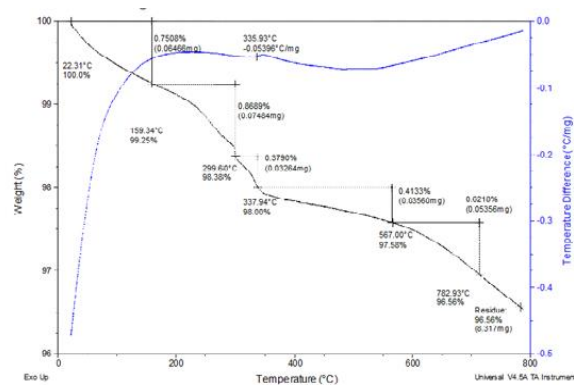


Figure 7. TGA/DSC image of NiO-CuO nanocomposite

#### 4. Conclusion

In summary, NiO-CuO nanocomposite was prepared by the Sol-Gel method. The XRD pattern indicates the formation of the mixed coupled phase (cubic-monoclinic) of NiO-CuO having particle size about 25 nm. The SEM results have shown that the average crystallite size and agglomeration increase with an increase in the calcination temperature, which can be attributed to the improvement in the crystallinity of the samples. TEM analysis shows the existence of spherical and cubic structure of NiO-CuO nanocomposite. It is also clear that the mean particle size estimated by TEM is in good agreement with the average crystallite size determined from the XRD data. The EDX spectra confirm the presence of Ni, Cu and O of elements without any other impurity species. UV-Visible study indicated the occurrence of both direct optical transition and indirect optical transition. Our study confirms that by making composite with CuO has influenced significantly on the crystallite size and strain of NiO nanoparticles. FTIR spectra have confirmed the establishment of CuO nanoparticles. The peak of Cu-O stretching was observed at  $657.13\text{ cm}^{-1}$  for NiO-CuO nanocomposite due to the presence of Cu-O bond. The thermal analysis of NiO-CuO was directly towards the oxidation and cracking-combustion behaviour and even further kinetic analysis were determined by using differential scanning calorimetry (DSC) and thermo gravimetric analysis-differential thermal analysis (TGA-DTA).

#### Acknowledgments

The authors are gratefully acknowledges to the Institute of Tatyasaheb Kore Institute of Engineering and Technology Warananagar, and Yashwantrao Chavan WaranaMahavidyalaya, Warananagar, Maharashtra, India for providing laboratory facilities.

#### References

- [1] U. J. Tupe, M. S. Zambare, A. V. Patil and P. B. Koli, "The Binary Oxide NiO-CuO Nanocomposite Based Thick Film Sensor for the Acute Detection of Hydrogen Sulphide Gas Vapours," *Mat. Sci. Res. India*, 2020, Vol. 17(3), pp. 260-269.
- [2] T. T. Bhosale, H. M. Shinde, N. L. Gavade, S. B. Babar, V. V. Gawade, S. R. Sabale · R. J. Kamble, B. S. Shirke, K. M. Garadkar, "Biosynthesis of SnO<sub>2</sub> nanoparticles by aqueous leaf extract of *Calotropis gigantea* for photocatalytic applications," *J. Mater. Sci. Mater. Electron*, 2018, vol. 29(8).
- [3] A. Sharma, S. Kumar, N. Budhiraja, S. Dahiya and Mohan, "Effect of calcination on optical properties and morphology of NiO-CuO NanoComposites," *Singh Arch. Appl. Sci. Res.*, 2013, vol.5 (3), pp.122-128.
- [4] K. Ghanbari, Z. Babaei, "Fabrication and characterization of non-enzymatic glucose sensor based on ternary NiO/CuO/polyaniline nanocomposite," *Analytical Biochemistry*, 2016.
- [5] B. S. Shirke, A. A. Patil, P. P. Hankare, K. M. Garadkar, "Synthesis of cerium oxide nanoparticles by microwave technique using propylene glycol as a stabilizing agent," *J. Mater. Sci: Mater Electron*. 2011, vol. 22, pp. 200–203.

- [6] K. M. Garadkar, B. S. Shirke, Y. B. Patil and D. R. Patil, "Nanostructured ZrO<sub>2</sub> Thick Film Resistors as H<sub>2</sub>-Gas Sensors Operable at Room Temperature," *Sensors & Transducers J.*, 2009, vol.110(11), pp.17-25.
- [7] P. Mallick, C. S. Sahoo, "Effect of CuO Addition on the Structural and Optical Properties of NiO Nanoparticles," *Nanoscience and Nanotechnology*, 2013, vol. 3(3), pp.52-55.
- [8] A.O. Juma, E.A.Arbab, C.M. Muiva, L.M. Lepodise, G.T. Mola, "Synthesis and characterization of CuO-NiO-ZnO mixed metal oxide nanocomposite," *J. Alloy.Comp.*, 2017.
- [9] T. T. Bhosale, A. R. Kuldeep, S. J. Pawar, B. S. Shirke, K. M. Garadkar, "Photocatalytic degradation of methyl orange by Eu doped SnO<sub>2</sub> nanoparticles," *J.Mat. Sci. Mat. Elect.* 2019, vol. 30(20), pp.18927-18935.
- [10] Abd El-Aziz A.Said, Mohamed M. Abd El-Wahab, Soliman A. Soliman, Mohamed N. Goda "Synthesis and Characterization of Nano CuO-NiO Mixed Oxides," *Nanoscience and Nanoengineering* 2014, vol. 2(1), pp.17-28.
- [11] G. K. Weldegebrual, "Photocatalytic and antibacterial activity of CuO nanoparticles biosynthesized using *Verbascum thapsus* leaves extract," *Optik-International J.Light and Electron Optics*, 2020, vol. 204, pp.164230.
- [12] T. H. Tran and V. T. Nguyen, "Copper Oxide Nanomaterials Prepared by Solution Methods, Some Properties and Potential Applications: A Brief Review," *International Scholarly Research Notices Volume* 2014, Article ID 856592, pp.14.
- [13] X. Zhao, P. Wang, Z. Yan, N. Ren, "Room temperature photoluminescence properties of CuO nanowire arrays," *J. Opt. Mater.* 2015, vol.42, pp.544-547.
- [14] M. Bonomo, "Synthesis and Characterization of NiO Nanostructures: a Review " *J.Nanoparticle Res* 2018, vol.20(8), pp.222.
- [15] A. Rahdar, M. Aliahmad and Y. Azizib, "NiO Nanoparticles: Synthesis and Characterization," *JNS* 2015, vol.5, pp.145-151.
- [16] Shamim, Z. Ahmad, S. Mahmood, U.Ali, T. Mahmood and Z. Nizami, "Synthesis of nickel nanoparticles by sol-gel method and their characterization," *Open J. Chem.* 2019, vol. 2(1), pp.16-20.
- [17] S. Zahra, N. Naz, M. Zia-ur-Rehman, M. Irfan, A. Sheikh and S.Izhar, "Characterization of Sol-gel Prepared Silica Supported NiO-CuO Composites," *J. Chem. Soc. Pak.*, 2020, vol.42(2), pp.164-170.
- [18] S. Chatterjee, A. Ray, M. Mandal, S. Das, and S. K. Bhattacharya, "Synthesis and Characterization of CuO-NiO Nanocomposites for Electrochemical Supercapacitors," *JMEPEG* 2020, vol.29(12), pp.8036-8048.
- [19] L. Argueta-Figueroa, "Synthesis, characterization and antibacterial activity of copper, nickel and bimetallic Cu-Ni nanoparticles for potential use in dental materials," *Progress in Natural Science: Materials International* 2014, vol.24(4), pp.321-328.